

Gammaherpesvirus Small Noncoding RNAs Are Bifunctional Elements That Regulate Infection and Contribute to Virulence *In Vivo*

Kevin W. Diebel,^{a*} Lauren M. Oko,^a Eva M. Medina,^a Brian F. Niemeyer,^a Cody J. Warren,^a David J. Claypool,^{a*} Scott A. Tibbetts,^b Carlyne D. Cool,^{c,d} Eric T. Clambey,^e Linda F. van Dyk^a

Department of Immunology & Microbiology, University of Colorado School of Medicine, Aurora, Colorado, USA^a; Department of Molecular Genetics & Microbiology, University of Florida College of Medicine, Gainesville, Florida, USA^b; Division of Pulmonary and Critical Care Medicine, Department of Medicine,^c Department of Pathology,^d and Department of Anesthesiology,^e University of Colorado School of Medicine, Aurora, Colorado, USA

* Present address: Kevin W. Diebel, Biomedical Sciences Department, University of Minnesota Medical School Duluth, Duluth, Minnesota, USA; David J. Claypool, Department of Pediatrics, University of Colorado School of Medicine, Aurora, Colorado, USA.

K.W.D. and L.M.O. contributed equally to this work.

ABSTRACT Many viruses express noncoding RNAs (ncRNAs). The gammaherpesviruses (γ HVs), including Epstein-Barr virus, Kaposi's sarcoma-associated herpesvirus, and murine γ HV68, each contain multiple ncRNA genes, including microRNAs (miRNAs). While these ncRNAs can regulate multiple host and viral processes *in vitro*, the genetic contribution of these RNAs to infection and pathogenesis remains largely unknown. To study the functional contribution of these RNAs to γ HV infection, we have used γ HV68, a small-animal model of γ HV pathogenesis. γ HV68 encodes eight small hybrid ncRNAs that contain both tRNA-like elements and functional miRNAs. These genes are transcribed by RNA polymerase III and are referred to as the γ HV68 TMERs (tRNA-miRNA-encoded RNAs). To determine the total concerted genetic contribution of these ncRNAs to γ HV acute infection and pathogenesis, we generated and characterized a recombinant γ HV68 strain devoid of all eight TMERs. TMER-deficient γ HV68 has wild-type levels of lytic replication *in vitro* and normal establishment of latency in B cells early following acute infection *in vivo*. In contrast, during acute infection of immunodeficient mice, TMER-deficient γ HV68 has reduced virulence in a model of viral pneumonia, despite having an enhanced frequency of virus-infected cells. Strikingly, expression of a single viral tRNA-like molecule, in the absence of all other virus-encoded TMERs and miRNAs, reverses both attenuation in virulence and enhanced frequency of infected cells. These data show that γ HV ncRNAs play critical roles in acute infection and virulence in immunocompromised hosts and identify these RNAs as a new potential target to modulate γ HV-induced infection and pathogenesis.

IMPORTANCE The gammaherpesviruses (γ HVs) are a subfamily of viruses associated with chronic inflammatory diseases and cancer, particularly in immunocompromised individuals. These viruses uniformly encode multiple types of noncoding RNAs (ncRNAs) that are not translated into proteins. It remains unclear how virus-expressed ncRNAs influence the course and outcome of infection *in vivo*. Here, we generated a mouse γ HV that lacks the expression of multiple ncRNAs. Notably, this mutant virus is critically impaired in the ability to cause disease in immunocompromised hosts yet shows a paradoxical increase in infected cells early during infection in these hosts. While the original mouse virus encodes multiple ncRNAs, the expression of a single domain of one ncRNA can partially reverse the defects of the mutant virus. These studies demonstrate that γ HV ncRNAs can directly contribute to virus-induced disease *in vivo* and that these RNAs may be multifunctional, allowing the opportunity to specifically interfere with different functional domains of these RNAs.

Received 22 July 2014 Accepted 28 December 2014 Published 17 February 2015

Citation Diebel KW, Oko LM, Medina EM, Niemeyer BF, Warren CJ, Claypool DJ, Tibbetts SA, Cool CD, Clambey ET, van Dyk LF. 2015. Gammaherpesvirus small noncoding RNAs are bifunctional elements that regulate infection and contribute to virulence *in vivo*. *mBio* 6(1):e01670-14. doi:10.1128/mBio.01670-14.

Editor Rozanne M. Sandri-Goldin, University of California, Irvine

Copyright © 2015 Diebel et al. This is an open-access article distributed under the terms of the [Creative Commons Attribution-Noncommercial-ShareAlike 3.0 Unported license](https://creativecommons.org/licenses/by-nc-sa/4.0/), which permits unrestricted noncommercial use, distribution, and reproduction in any medium, provided the original author and source are credited.

Address correspondence to Linda F. van Dyk, Linda.VanDyk@ucdenver.edu.

The gammaherpesviruses (γ HVs) are a subfamily of large, double-stranded DNA viruses that include the human pathogens Epstein-Barr virus (EBV, human herpesvirus 4 [HHV-4]) and Kaposi's sarcoma-associated herpesvirus (KSHV, HHV-8), the primate virus herpesvirus saimiri (HVS, SaHV-2), and murine γ HV68 (also known as murine herpesvirus 68 or murid herpesvirus 4). These viruses establish a lifelong infection of their hosts, with long-term latency in lymphocytes (1). While γ HVs are typi-

cally controlled in healthy, immunocompetent individuals, these viruses are associated with the development of multiple pathologies, including malignancies, in immunocompromised individuals (2).

The γ HVs contain a wide variety of genes, including many noncoding RNAs (ncRNAs) (3). γ HV ncRNAs range from nuclear ncRNAs (e.g., EBV-encoded small RNAs [EBERs], KSHV polyadenylated nuclear RNA [PAN RNA], and HVS U RNAs

[HSURs]) to functional miRNAs (3–11). ncRNAs have been shown to regulate a number of cellular and viral processes, with recent studies particularly focused on how viral miRNAs modulate the outcome of infection (12, 13). While viral miRNAs can modulate diverse processes, multiple reports have identified the capacity of these miRNAs to autoregulate viral gene expression during lytic and latent infections and to alter host gene expression (e.g., to promote immune evasion).

Despite major advances in the understanding of γ HV miRNAs, the genetic contribution of viral ncRNAs to primary infection and pathogenesis *in vivo* remains largely unknown. While there is evidence that γ HV ncRNAs can contribute to various stages of infection, including lymphocyte transformation *in vitro* and regulation of lytic replication *in vitro* (14–17), roles for viral ncRNAs in many aspects of infection have been more difficult to ascertain by available assays (18–20). Importantly, the strict species specificity of the human γ HVs has impeded the understanding of the role of viral ncRNAs during primary infection *in vivo*.

γ HV68 is a close genetic relative of the other γ HVs and is now a well-established small-animal model used to study γ HV pathogenesis (21). A major strength of this model is the ability to analyze the full course of infection *in vivo*, from acute infection to long-term maintenance of latency and reactivation from latency. Similar to the human γ HVs, γ HV68 establishes latency in B cells, with latency also found in macrophages, dendritic cells, and possibly epithelial cells (21); γ HV68 can spontaneously reactivate from latency *ex vivo*. Like the human γ HVs, γ HV68 induces chronic diseases, ranging from B cell tumors to chronic inflammatory diseases, in immunocompromised individuals (21). Given the genetic tractability of γ HV68 and its ability to infect inbred and genetically modified mice, this model has become a powerful system used to study factors that regulate γ HV pathogenesis.

Early studies of γ HV68 revealed the presence of eight tRNA-like ncRNAs that were clustered in a 6-kb region at the left end of the genome (22). Despite their sequence similarity to eukaryotic tRNAs, these viral tRNA-like RNAs (vtRNAs) were not aminoacylated, suggesting that they would not actively function as charged tRNAs (22). More recently, we and others found that γ HV68 encodes at least 15 *bona fide* microRNAs (miRNAs) (6, 10, 11) and that these miRNAs are cotranscribed with the vtRNAs from RNA polymerase III (Pol III)-dependent promoters (23). Given the hybrid nature of these transcripts and their similarity to the EBERs, we refer to these tRNA-miRNA-encoded RNAs as the γ HV68 TMERs (24). Though studies have revealed basic mechanisms that facilitate the production of mature miRNAs from these transcripts (24, 25), how these ncRNAs contribute to γ HV68 infection and pathogenesis remains poorly defined. Here, we report the characterization of a recombinant γ HV68 rendered deficient in the expression of all eight TMER genes. Through characterization of this mutant virus, we found that the γ HV68 TMERs are dispensable for lytic replication and the establishment of latency. However, the TMERs have a profound role in constraining the frequency of virus-infected cells during acute infection of immunocompromised hosts. Despite an exaggerated frequency of virus-infected cells upon ablation of the γ HV68 TMERs, TMER-deficient γ HV68 is significantly impaired in pathogenesis in immunocompromised hosts. These data provide evidence that γ HV ncRNAs actively shape the course of viral infection *in vivo*.

RESULTS

Features of the γ HV68 TMER coding locus. γ HV68 encodes eight RNA Pol III-transcribed TMERs within a region of the γ HV68 genome including nucleotide positions 127 to 5585, interspersed among two protein-coding genes, *M1* and *M2* (Fig. 1A). While early studies found that this region produced vtRNA elements (22), subsequent studies found that the TMER genes produce hybrid transcripts with a 5' vtRNA followed by one or more 3' miRNA-containing hairpins (6, 23, 25) (Fig. 1B). Transcription of the TMERs is dependent on RNA Pol III, and during viral infection, TMER-derived miRNAs are processed and functional (23).

The hybrid nature of the TMERs raised the possibility that the TMERs may function through both vtRNA- and miRNA-dependent mechanisms. Additionally, transcription of the TMER genes may play roles in epigenetic control of viral gene expression. In order to define the total genetic contribution of both TMER-derived vtRNA and miRNA elements during infection, we sought to disrupt all eight TMER genes. Instead of a straight deletion of each of the TMER genes, we built on our previous observation that transcription of the TMERs is absolutely dependent on an intact RNA Pol III promoter (23, 24, 26). On the basis of this insight, we systematically deleted each TMER Pol III promoter sequence, a mutation typically spanning 56 to 68 bp within the 5' end of each TMER. These mutations were engineered into a plasmid containing the native γ HV68 TMER locus (pLE-WT) to generate a modified TMER locus in which all TMER promoter elements were disrupted (pLE-TKO, for total knockout) (Fig. 1C).

To generate γ HV68 recombinants lacking the expression of all eight TMERs, we next used bacterial artificial chromosome (BAC)-based recombination employing a two-step Red-mediated recombination protocol (27, 28). By using the pLE-TKO plasmid as a recombination substrate, we generated TMER total-knockout (TMER-TKO) γ HV68 strains in two different backgrounds, (i) a wild-type (WT) γ HV68 BAC (29) and (ii) a WT γ HV68 BAC containing an open reading frame 73 (ORF73) β -lactamase fusion gene, referred to here as γ HV68. β la (30). Notably, γ HV68. β la-derived viruses express β -lactamase enzymatic activity at all stages of infection, allowing virus-infected cells to be identified by virtue of β -lactamase-mediated cleavage of a cell-permeating fluorescent substrate (30). The TMER-TKO mutations in the WT and WT β la backgrounds were generated independently and analyzed in parallel throughout this study. The predicted genomic structure of the TMER-TKO mutation is presented in Fig. 2A, with verification of the TMER-TKO mutant done by (i) restriction digest analysis of intact BAC DNA (Fig. 2B), (ii) restriction digest analysis of a PCR product amplified from BAC DNA of the left end of the γ HV68 genome (Fig. 2C), and (iii) direct sequencing of the left end of the BAC DNAs. Following confirmation of these mutations, we generated the TMER-TKO viruses (see Materials and Methods).

We previously found that disruption of the TMER promoters prevented TMER expression following plasmid transfection (23). To verify that these mutations had a similar effect on TMER expression during virus infection, we measured the expression of the TMER-derived miRNAs and TMERs in the TMER-TKO. To measure TMER-derived miRNA expression, we used RNA ligation-mediated reverse transcription-PCR (RLM-RT-PCR) to detect mature miRNAs (23, 24). Whereas WT virus-infected cells had

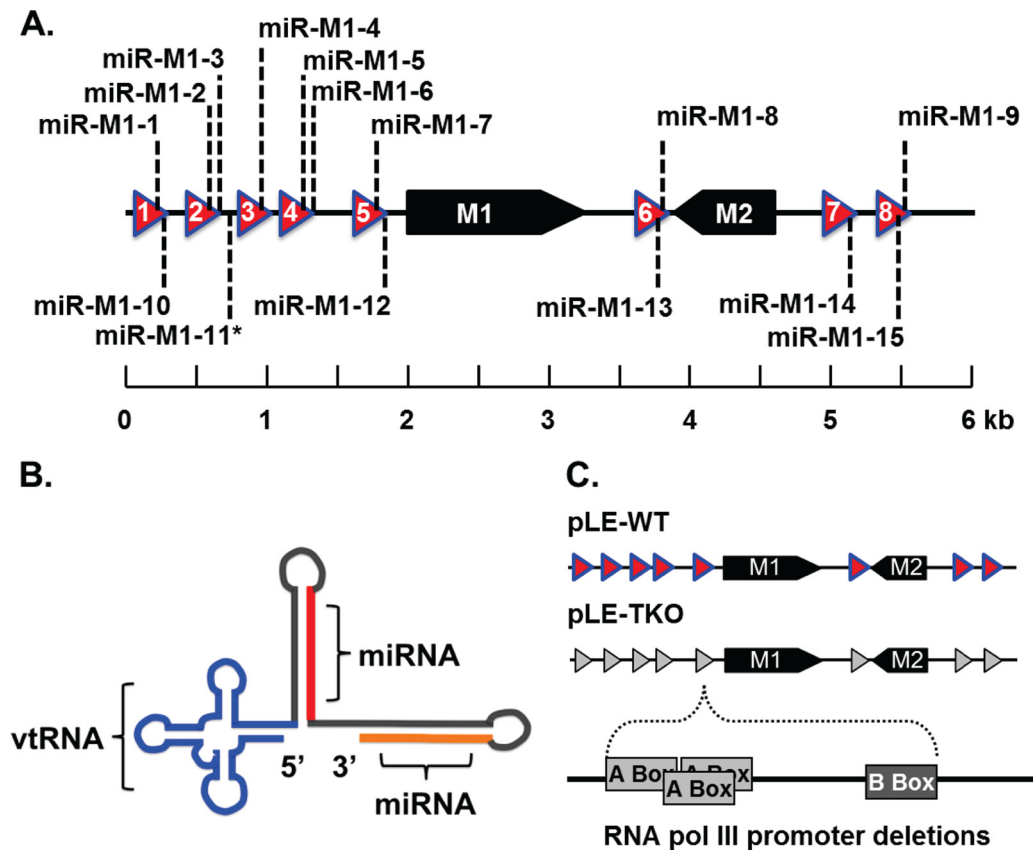


FIG 1 Genomic organization of the γ HV68 TMER genes and TMER mutagenesis strategy. (A) Genetic details of the left end of the γ HV68 genome. The TMER genes are represented as colored triangles numbered 1 through 8. The ORFs for *M1* and *M2* are shown as black arrows. Locations of the γ HV68 miRNA genes are shown as dashed lines and numbered miR-M1-1 through -15. *miR-M1-11 is the only γ HV68 miRNA not directly embedded within a TMER primary transcript (10, 11). miRNA genes are named according to the miRBase nomenclature (49). (B) Schematic of a single TMER (TMER1) identifying the vtRNA- and miRNA-containing stem-loops. (C) Schematics of the γ HV68 genomic inserts in the pLE-WT and pLE-TKO plasmids (23). The grayed-out triangles in the pLE-TKO insert represent TMER genes for which the RNA Pol III promoter sequences have been deleted. Shown below the pLE-TKO schematic is a generic representation of the RNA Pol III promoter region removed from each γ HV68 TMER gene.

detectable expression of multiple TMER-derived miRNAs, TMER-TKO virus-infected cells had no detectable miRNA expression (Fig. 3A). RLM-RT-PCR detection of the cellular miRNA mmu-miR-21 indicated that miRNA recovery and preparation were efficient and equivalent across all of the samples (Fig. 3A). These data demonstrate that TMER-TKO γ HV68 fails to express TMER-derived miRNAs.

To determine if any RNA species was being transcribed from the TMERs in the TMER-TKO virus, we performed northern blot analysis of RNAs from WT and TMER-TKO virus-infected cells. While WT virus-infected cells showed the expression of multiple TMER-derived elements (including primary miRNAs [pri-miRNAs]- and pre-miRNAs), TMER-TKO virus-infected cells had no detectable expression of TMER-derived elements (Fig. 3B). In total, these studies revealed that the TMER-TKO mutation specifically and efficiently prevents the expression of the TMERs and all TMER-associated elements.

The TMERs are interspersed among the *M1*, *M2*, and *M3* protein-coding genes. To verify the specificity of the TMER-TKO and to determine whether deletion of the ~60-bp TMER promoters (and thus lack of Pol III binding and transcription) could alter the expression of these neighboring genes, we measured the expression of *M1*, *M2*, *M3*, and Rta/ORF50 by RT-PCR and quanti-

tative real-time PCR (Fig. 3C and D). This analysis showed mRNA levels for each of these viral genes that were comparable in the WT and TMER-TKO viruses. These data indicate that deletion of the TMER promoter elements specifically prevents transcription of the TMERs while having no effect on the expression of neighboring protein-coding genes, including *M1*, *M2*, or *M3*.

Lytic replication of γ HV68 TMER-TKO. The ability to generate and amplify the TMER-TKO virus indicated that the TMERs are not essential for lytic replication, a finding consistent with previous reports of γ HV68 variants lacking the TMER locus and neighboring genes (31, 32). To determine the effect of the TMERs on lytic infection *in vitro*, we measured virus production in either single or multiple rounds of replication by using either a high or a low multiplicity of infection (MOI), respectively. This analysis compared the replication of both γ HV68- and γ HV68. β -derived TMER-TKO recombinants. While we noted minor differences at intermediate time points, including some with statistical significance, these studies revealed that ablation of the γ HV68 TMERs had a negligible impact on replication fitness *in vitro* (Fig. 4). Further, both single-step and multistep replications were independent of the TMERs in interferon (IFN)-deficient BHK cells (data not shown). Our data indicate that the TMERs are genetically dispensable for lytic replication *in vitro*.

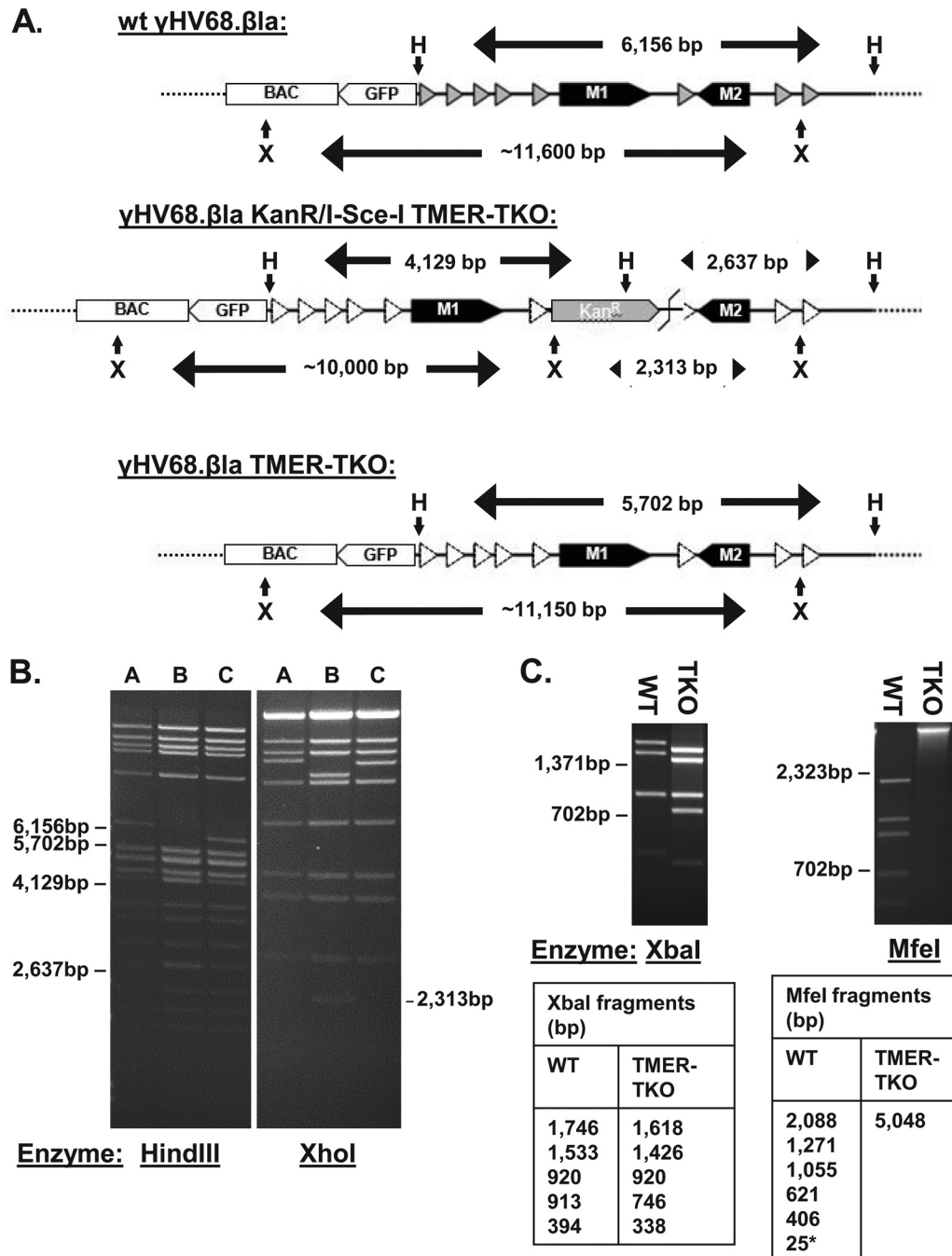


FIG 2 γ HV68 TMER-TKO mutant construction. (A) Schematic showing the genomic organization of the γ HV68 TMER locus in the BAC DNAs for parental WT γ HV68. β la, intermediate viral recombinant γ HV68. β la Kan^r/I-Sce-I TMER-TKO (for antibiotic selection in bacteria), and γ HV68. β la TMER-TKO (in which the Kan^r-encoding gene is removed). TMERs are indicated by gray triangles in WT γ HV68 and as white triangles indicating the deletion of RNA Pol III promoter elements in the TMER-TKO recombinants. Restriction enzyme sites (H for HindIII, X for XhoI) and distances between these sites are indicated. (B) Agarose gel electrophoresis of restriction digests of BAC DNA for WT γ HV68. β la (lane A), γ HV68. β la Kan^r/I-Sce-I TMER-TKO (lane B), and γ HV68. β la TMER-TKO (lane C) following digestion with HindIII (left) or XhoI (right). (C) Agarose gel electrophoresis of restriction digests of PCR amplicons from the WT γ HV68. β la and γ HV68. β la TMER-TKO following digestion with XbaI (left) or MfeI (right). Predicted sizes of restriction digest fragments are indicated. The 25-bp MfeI fragment of the WT γ HV68. β la PCR amplicon cannot be visualized on this gel. Molecular size markers are shown beside each gel.

Infection of immunocompetent mice with the γ HV68 TMER-TKO. We next analyzed TMER-TKO acute infection in WT, immunocompetent hosts (C57BL/6) [B6] mice. WT and TMER-TKO virus-infected mice showed comparable splenomegaly at 14 days postinfection (p.i.) (Fig. 5A). To determine the fre-

quency of virus-infected cells, we next infected B6 mice with the WT γ HV68. β la and γ HV68. β la TMER-TKO viruses. At 14 days p.i., splenocytes were harvested from infected mice and samples were incubated with the fluorescent β -lactamase substrate CCF2-AM; this was followed by flow cytometric detection of the

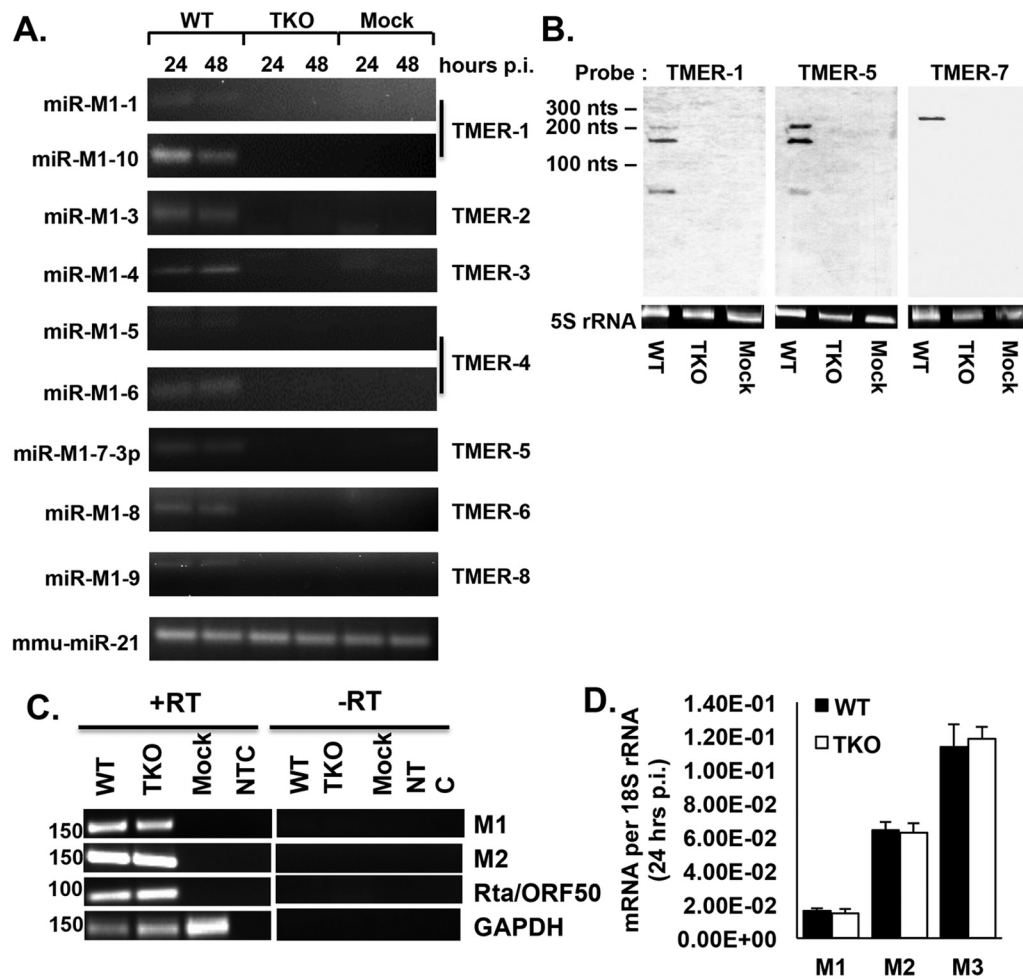


FIG 3 Validation of the γ HV68 TMER-TKO RNA analysis of WT and TMER-TKO virus-infected samples demonstrates that the TMER-TKO virus completely and specifically ablates transcription of the TMERs with no effect on neighboring genes. (A) RLM-RT-PCR analysis of mature miRNAs from total RNA isolated from WT or TMER-TKO (TKO) virus- or mock-infected 3T12 cells (MOI of 5) at 24 or 48 h p.i. miRNAs are identified to the left of the gels, and the associated TMERs are identified on the right. TMER-TKO virus-infected samples uniformly failed to express viral miRNAs. mmu-miR-21 is a host miRNA to control for miRNA detection in all the samples. (B) Northern blot analysis for TMER1, TMER5, and TMER7 from total RNA isolated from WT or TKO virus-infected or mock-infected 3T12 cells (MOI of 5) at 24 h p.i. Ethidium bromide-stained 5S rRNA (shown below the blots) served as a loading control. TMER1 and TMER5 have an alternative termination site after the first hairpin that results in two different sizes of pri-miRNA products, where TMER7 does not and results in only one band for the pri-miRNA. TKO virus-infected samples had undetectable expression of TMER1, -5, and -7. (C) RT-PCR analysis for the γ HV68 M1, M2, and Rta/ORF50 transcripts with total RNA isolated from WT or TKO virus- or mock-infected 3T12 cells (MOI of 5) at 24 h p.i. A no-template control (NTC) was included. Amplification occurred only in the presence of reverse transcriptase (+RT), demonstrating that all amplifications reflect detection of RNA and not genomic DNA. (D) Quantitative RT-PCR analysis of the γ HV68 M1, M2, and M3 transcripts from total RNA isolated from WT and TKO virus-infected 3T12 cell samples at 24 h p.i. All quantifications are standardized relative to 18S rRNA levels.

β -lactamase-cleaved substrate (which emits fluorescence at 447 nm) (30). This analysis revealed that the WT and TMER-TKO viruses both infected CD19⁺ B cells (Fig. 5B). When we analyzed the properties of virus-infected cells, WT and TMER-TKO virus-infected B cells both showed increased cell size (forward scatter [FSC]), increased granularity (side scatter [SSC]), and downregulation of surface IgD expression (Fig. 2C) relative to B cells in mock-infected mice. These data suggest that both the WT and TMER-TKO viruses have the capacity to infect activated B cells undergoing the process of isotype class switching, consistent with previous studies of γ HV68 latency (33, 34). While the frequencies of infection with the WT and TMER-TKO viruses, defined by β -lactamase-expressing (β la⁺) cells, were similar, there was a slight increase in the frequency of TMER-TKO virus-infected cells

at 14 days p.i. (Fig. 5D and E), an observation also noted at 21 days p.i. (data not shown).

The γ HV68 TMERs are required for optimal virulence in acute viral pneumonia in immunocompromised mice. WT γ HV68 causes acute lethal pneumonia in BALB.IFN- γ ^{-/-} mice (35). Whereas mice infected with WT γ HV68 had an ~60 to 80% mortality rate by 14 days p.i., mice inoculated with γ HV68 Δ 9473 (31) (a virus with a 9,473-bp deletion that removes all eight TMERs, M1, M2, M3, and part of M4) was fully attenuated in pathogenesis (Fig. 6A). To determine the specific contributions of the TMERs to pathogenesis in this model, we compared the relative abilities of the WT and TMER-TKO viruses to induce pneumonia. In contrast to WT virus-infected mice, which showed progressively increasing disease severity and developed pneumonia

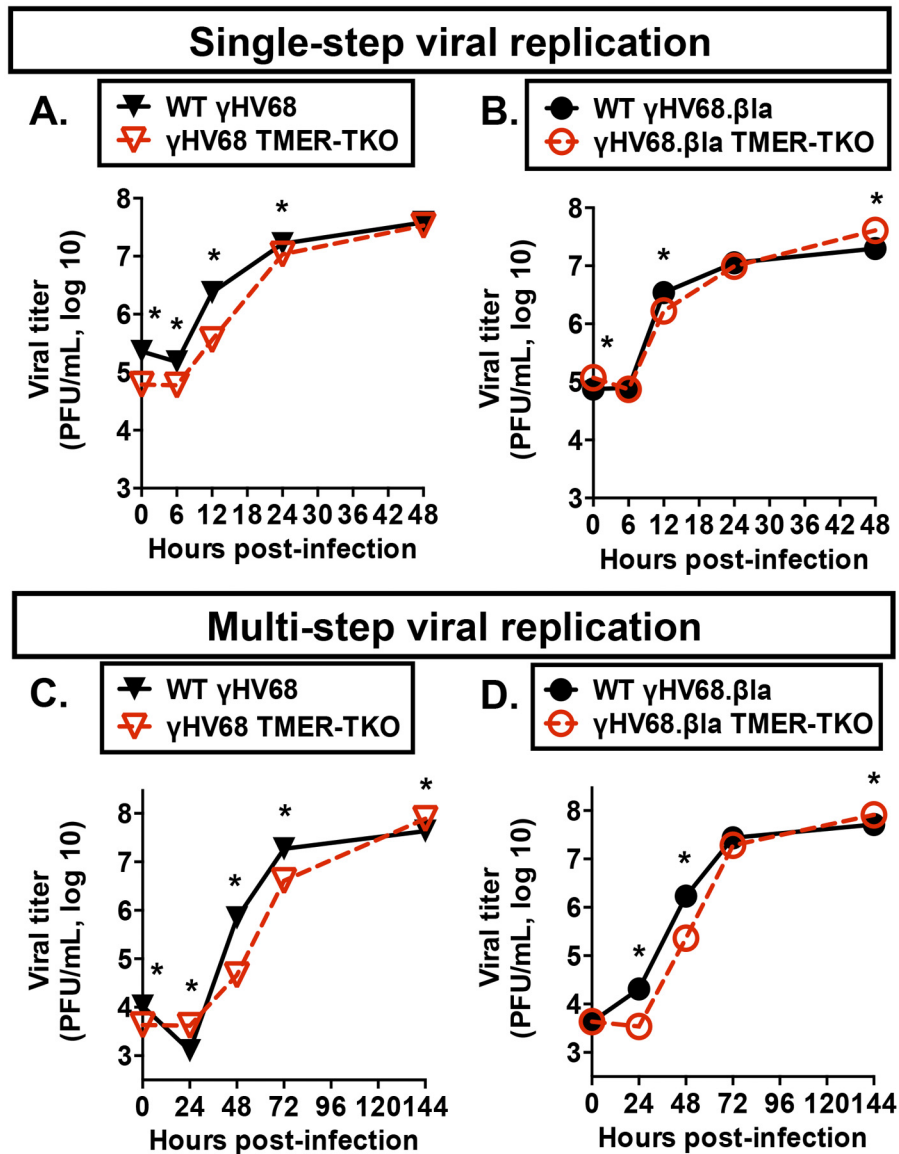


FIG 4 The γ HV68 TMERs are dispensable for *in vitro* replication in fibroblasts. Analysis of single (A and B) and multiple (C and D) rounds of viral replication in 3T12 fibroblasts, comparing infection with the WT γ HV68 and γ HV68 TMER-TKO viruses (A and C) and infection with the WT γ HV68. β la and γ HV68. β la TMER-TKO viruses that contain the ORF73- β la reporter gene (B and D). (A and B) Single-step replication analysis with WT (black filled symbols) or TMER-TKO (open red symbols) with cells infected at an MOI of 5. Cells and supernatants were collectively harvested at the postinfection times indicated. (C and D) Multistep replication analysis was done comparably to single-step analysis, with cells infected at an MOI of 0.05. Viral titers were assessed by plaque assay, and the data depict the mean \pm the standard error of the mean of three independent experiments, with one to three replicates per experiment. All plots include error bars; in cases where error bars are not shown, the standard error of the mean is very low. Statistically significant differences were calculated by unpaired t test comparing WT and TKO values at each individual time, and statistically significant differences are indicated (*, $P < 0.05$).

(Fig. 6C to F), mice infected with the TMER-TKO virus were characterized by an attenuated course of disease, as manifested by delayed death and a reduced mortality rate (Fig. 6A). While both WT and TMER-TKO virus-infected lungs had pronounced cellular infiltration and pulmonary inflammation, TMER-TKO virus-infected lungs tended to have a slightly higher prevalence of exudative infiltrates (Fig. 6D to G). Similar deficits of TMER-TKO viruses were observed in both the WT and WT γ HV68. β la backgrounds (Fig. 6A). In total, these data demonstrate that the γ HV68 TMERs are required for optimal pathogenesis in immunocompromised hosts.

Determination of the minimal genetic requirement sufficient to reverse the TMER-TKO deficit. The γ HV68 TMER-TKO virus lacks transcription from all 8 TMER genes, ablating the production of 8 TMER-derived vRNAs and 15 TMER-derived miRNAs. While the hybrid nature of the TMERs suggests that both vRNAs and miRNAs may contribute to γ HV68 infection, one notable difference between the vRNAs and the miRNAs is their conservation. While the vRNAs are remarkably similar to one another in sequence and structure, the final processed miRNAs have distinct sequences and therefore likely possess specific and unique biological functions.

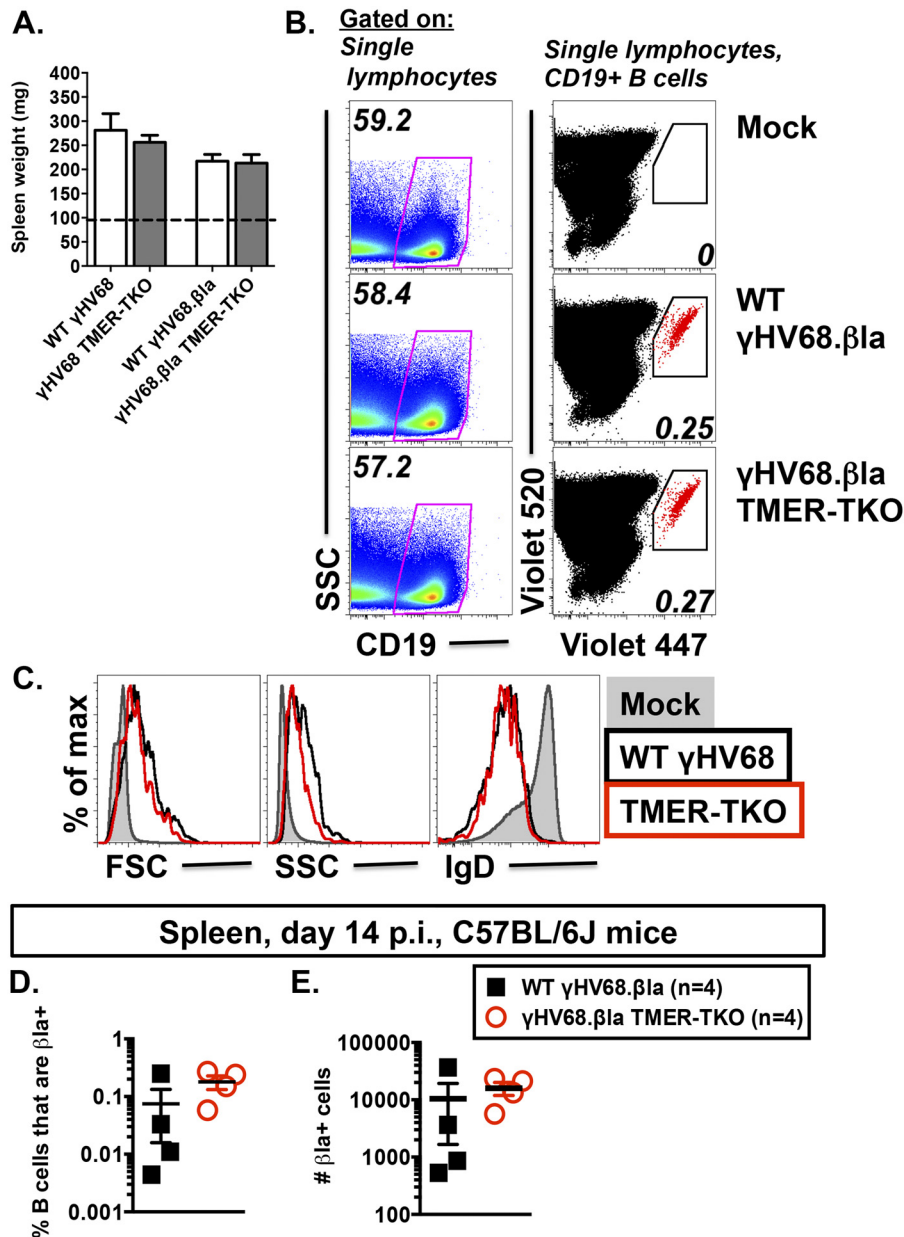


FIG 5 The γ HV68 TMERs are dispensable for the establishment of latent infection of B cells in B6 mice. B6 mice were infected with either WT or TMER-TKO virus as indicated and harvested at day 14 p.i. (A) Spleen weights of mice infected with the viruses indicated. Shown is the mean value \pm the standard error of the mean of five mice per group. (B) Representative flow cytometric analysis of cells from the spleens of B6 mice at day 14 p.i. comparing mock-infected samples and samples infected with the WT γ HV68.βla or γ HV68.βla TMER-TKO virus. Data depict the frequency of CD19⁺ B cells among lymphocytes that are single cells (left column) and the frequency of CD19⁺ B cells that are virus infected (βla-expressing cells), with βla⁺ cells identified in the top right quadrant and identified as red dots within the identified polygon (right column). (C) Analysis of cell size (FSC), granularity (SSC), and IgD expression comparing B cells from mock-infected spleen cells (gray) to WT γ HV68.βla (black) or γ HV68.βla TMER-TKO (red) virus-infected CD19⁺ βla⁺ B cells. (D and E) Quantitation of the frequency of virus-infected βla⁺ cells among CD19⁺ B cells (D) and the total number of virus-infected βla⁺ cells from WT γ HV68.βla (black) or γ HV68.βla TMER-TKO (red) virus-infected splenocytes (E). Each symbol indicates an individual mouse value, where horizontal black lines indicate the mean value \pm the standard error of the mean. The data in panels B to E are from two independent experiments with two mice per group per experiment.

To better understand which elements of the TMERs are required for optimal pathogenesis *in vivo*, we generated viral recombinants that contained either a single, intact TMER (γ HV68 TMER1 only) or expressed only the vtRNA module of TMER1 (γ HV68 vtRNA1 only, lacking the associated miRNA stem-loops). The γ HV68 vtRNA1 only was generated by insertion of a strong transcriptional terminator between the vtRNA and down-

stream miRNA elements (as described in Materials and Methods). Each of these recombinants has promoter deletions in the remaining TMERs, such that these viruses express only a single TMER (TMER1) or a single vtRNA (vtRNA1) (Fig. 7A).

Following generation and sequence confirmation of correct genomic targeting of these recombinants, we next sought to define the consequences of these mutations for TMER gene expression.

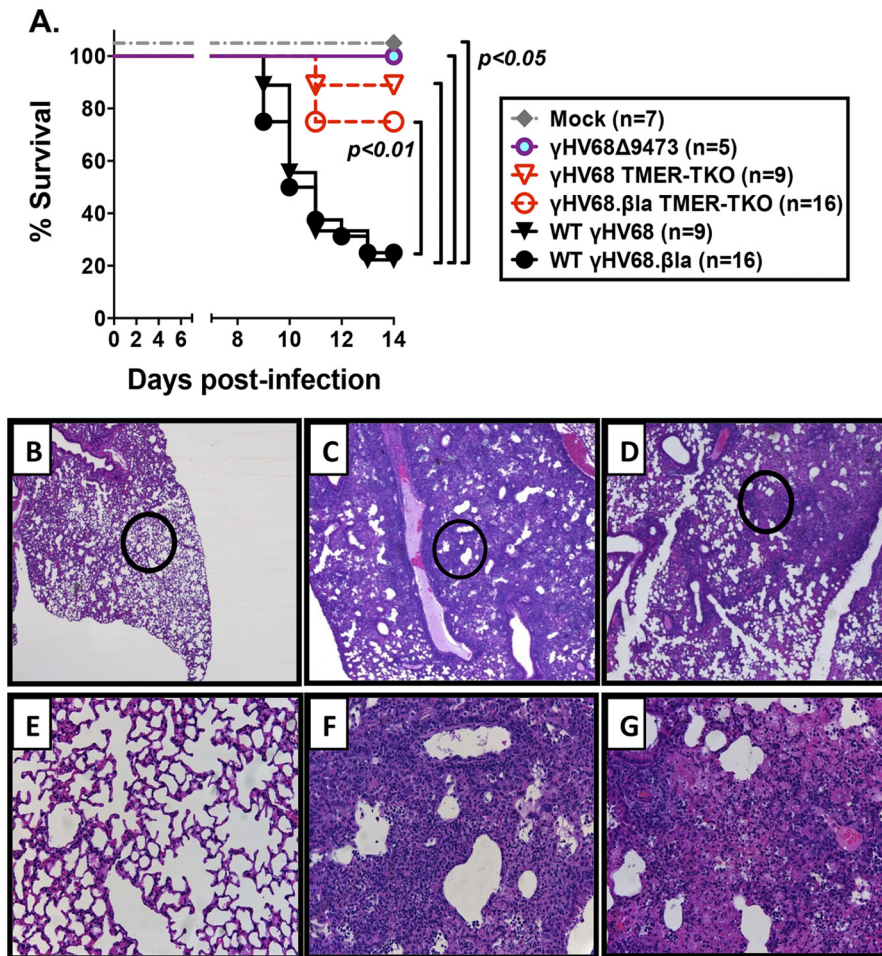


FIG 6 The γ HV68 TMERs are required for virulence in a model of acute lethal pneumonia in BALB.cIFN- $\gamma^{-/-}$ mice. (A) Survival of BALB.cIFN- $\gamma^{-/-}$ mice following infection with a series of viral recombinants. The survival of mock-infected mice (gray diamonds) is compared with that of mice infected with WT (closed black symbols) or TMER-TKO (open red symbols) γ HV68 with or without the β la reporter. γ HV68 Δ 9473 (gray circles) is a γ HV68 variant that lacks the entire TMER locus and the *M1*, *M2*, *M3*, and *M4* genes (31). The number of mice in each group is indicated in the box. Hematoxylin-and-eosin-stained lung tissue from mock-infected (B and E) and WT γ HV68. β la (C and F) and γ HV68. β la TMER-TKO (D and G) virus-infected mice at either low ($\times 40$, B to D) or high ($\times 200$, E to G [circled areas in panels B to D]) magnification. Lungs were harvested at 8 days p.i. from virus-infected mice and 14 days p.i. from mock-infected mice. In this model, 8 to 11 days p.i. is the peak of disease signs, where there is notable infiltration and severe pneumonia. Statistical analysis of survival curves was done by log-rank (Mantel-Cox) test performing pairwise comparisons of virus mutants relative to the appropriate WT control (WT γ HV68 or WT γ HV68. β la). Statistically significant differences from the WT are indicated.

To do this, we analyzed the expression of TMER-derived elements by northern blot analysis and found that the vtRNA1-only and TMER1-only viruses differ from the WT virus in that they lack TMERs 2 to 8 and express an increased level of TMER1 (Fig. 7B). As predicted, the vtRNA1-only virus transcribes the TMER1 gene only up to the intended insertion of two runs of *T*(6). This efficient termination signal limits TMER1 expression to the vtRNA module and the first alternative termination signal and prevents expression of the TMER1 stem-loops. The selection of this termination site is significant in that it is coincident with the first natural termination site in TMER1, ensuring that normal termination and RNase Z processing to produce the vtRNA-like element are intact.

Following validation of the TMER1-only and vtRNA1-only viruses, we tested the ability of these viral recombinants to induce disease in the pneumonia model. In contrast to the TMER-TKO deficit, we found that infection with either the γ HV68 TMER1-

only or the γ HV68 vtRNA1-only recombinant virus resulted in an intermediate phenotype, with reduced virulence relative to that of WT γ HV68 but increased virulence relative to that of the TMER-TKO viruses (Fig. 7B). These data indicate that virulence in this disease model does not require all of the TMERs. Given that the vtRNA1-only recombinant is phenotypically identical to the TMER1-only virus, these data further indicate that the expression of a single vtRNA, in the absence of all other TMER-derived vtRNAs and miRNAs, is sufficient to facilitate virulence *in vivo*.

We previously showed that the viral cyclin and *M11* genes of γ HV68 are required for optimal virulence in BALB.cIFN- $\gamma^{-/-}$ mice, a phenotype associated with reduced virus replication in infected lungs (35). To determine whether the TMER-TKO virus had a similar replication defect *in vivo*, we measured viral replication in the lungs at days 5 and 8 p.i. Notably, however, this analysis revealed that the TMER-TKO, TMER1-only, and vtRNA1-only viruses had titers comparable to those of the WT virus in infected

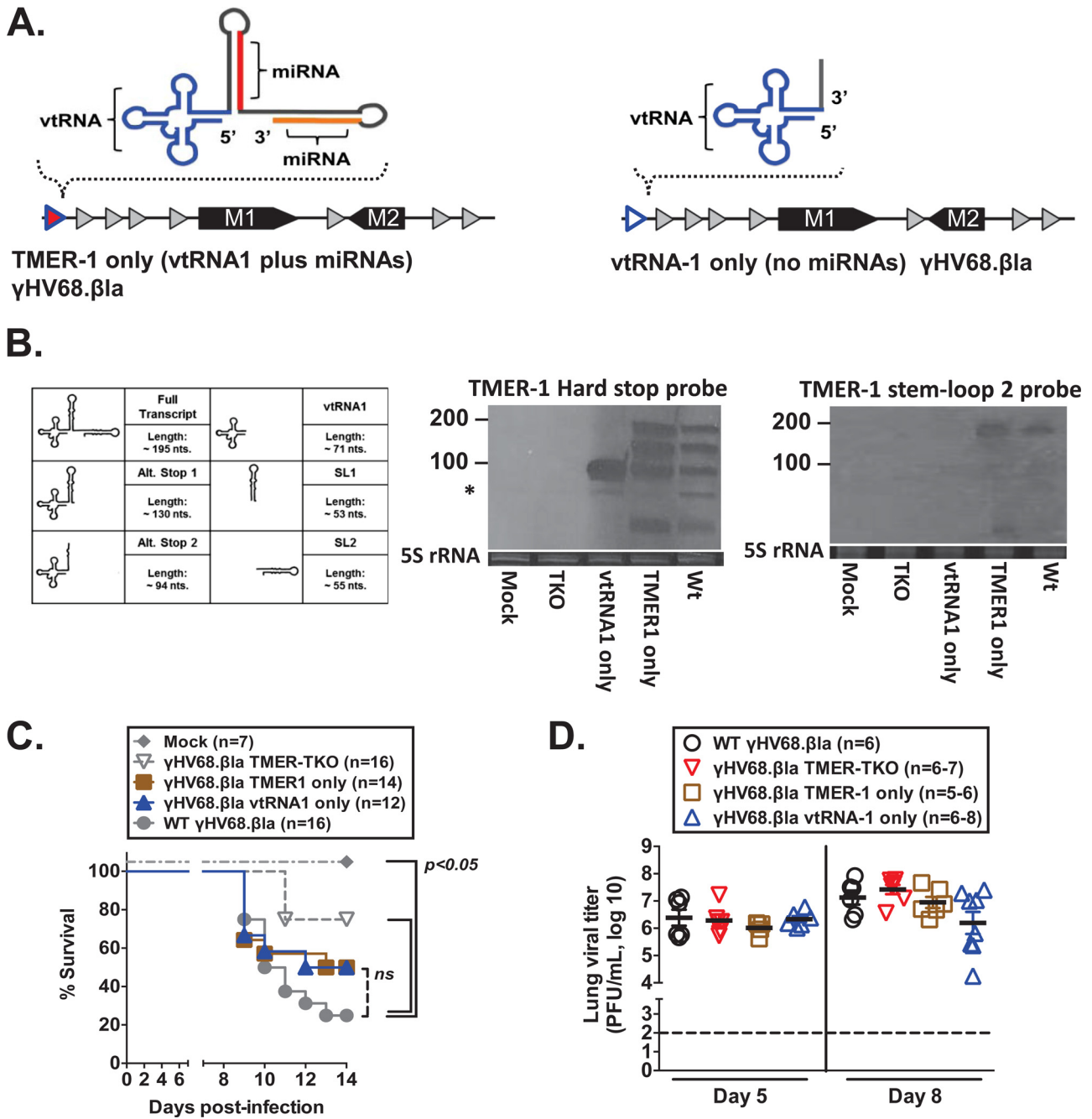


FIG 7 The γ HV68 TMER1-only and vtRNA1-only mutant viruses partially reverse the deficit of the γ HV68 TMER-TKO recombinant. (A) Schematic showing the genomic organization of the γ HV68 TMER locus in the γ HV68. β la TMER1-only and vtRNA1-only viruses. (B) Diagram of TMER-derived RNAs (left) and northern blot analysis of TMER1-derived products from WT, TMER-TKO (TKO), TMER1-only, or vtRNA1-only virus-infected or mock-infected 3T12 cells at 24 h p.i. (MOI of 5). Ethidium bromide-stained 5S rRNA (bottom) served as a loading control. Molecular size markers are indicated at the left; a nonspecific band is indicated by an asterisk. (C) Survival of BALB. $\text{IFN-}\gamma^{-/-}$ mice infected with γ HV68. β la TMER1-only (brown squares) and vtRNA1-only (blue triangles) recombinants, relative to that of mock-infected and WT γ HV68 and TMER-TKO virus-infected mice, indicated in gray (these data sets are the same data shown in Fig. 6A). *ns*, not significant. (D) Analysis of viral titers in the lungs of infected BALB. $\text{IFN-}\gamma^{-/-}$ mice at either day 5 (left) or day 8 (right) p.i. comparing WT and TMER mutant viruses, where each individual symbol represents a value from an individual mouse. The horizontal black lines indicate the mean titer of each group \pm the standard error of the mean. The horizontal dashed line at 2 PFU/ml indicates the limit of detection of the plaque assay. The number of mice per group is indicated. Statistical analysis of survival curves was done by log-rank (Mantel-Cox) test performing pairwise comparisons of mutant viruses and WT γ HV68. β la. Statistically significant differences from the WT are indicated. There were no statistically significant differences in virus titer as assessed by one-way ANOVA and Dunnett's multiple-comparison test, with all comparisons done relative to WT γ HV68. β la.

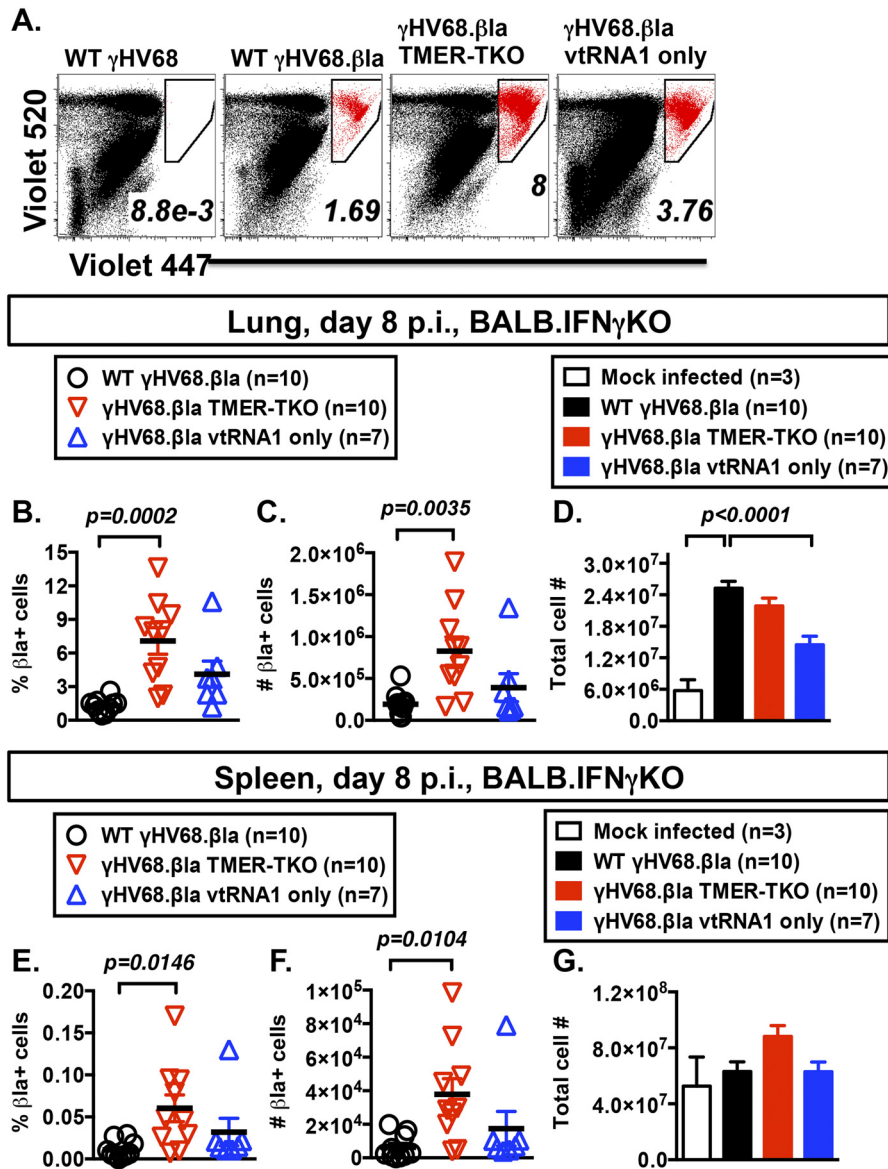


FIG 8 The γ HV68 TMERs limit the frequency of virus-infected cells in BALB.IFN- $\gamma^{-/-}$ mice. (A) Representative flow cytometric analysis of virus-infected cells from the lungs of infected BALB.IFN- $\gamma^{-/-}$ mice at day 8 p.i., as measured by the detection of β la-expressing cells, with β la⁺ cells identified in the top right quadrant as red dots within the identified polygon. Plots were gated by using a large gate based on cell size and granularity, followed by doublet exclusion. Quantitation of the frequency (B) and number (C) of β la⁺ cells in the lungs of mice at 8 days p.i. with WT γ HV68.βla, γ HV68.βla TMER-TKO, and γ HV68.βla vtRNA1-only viruses, with each symbol indicating an individual mouse value and horizontal black lines indicating the mean value \pm the standard error of the mean. (D) Total cellularity in lung tissue samples in panels B and C. Quantitation of the frequency (E) and number (F) of β la⁺ cells in the spleens of mice at 8 days p.i. with WT γ HV68.βla, γ HV68.βla TMER-TKO, and γ HV68.βla vtRNA1-only viruses. (G) Total cellularity in spleen tissue from samples in panels E and F. Data are from two or three independent experiments, with 7 to 10 mice per group. Statistical significance was assessed by one-way ANOVA and Dunnett's multiple-comparison test with adjusted *P* values as indicated; all comparisons were done relative to WT γ HV68.βla.

lungs at days 5 and 8 p.i. (Fig. 7C). These data indicate that the attenuation of the ability of the TMER-TKO mutant to induce viral pneumonia does not result from impaired viral replication *in vivo*.

The γ HV68 TMERs negatively regulate the frequency of virus-infected cells in immunodeficient mice. Despite the profound impairment of the ability of the TMER-TKO virus to induce lethal pneumonia in BALB.IFN- $\gamma^{-/-}$ mice, acute viral replication titers are comparable to those of the WT virus. To further characterize the status of infection in TMER-TKO virus-infected

mice, we quantified the frequency of virus-infected cells by flow cytometric analysis of β la⁺ cells in the lungs and spleens of infected BALB.IFN- $\gamma^{-/-}$ mice at day 8 p.i., comparing WT, TMER-TKO, and vtRNA1-only virus-infected mice. Whereas WT γ HV68.βla virus-infected mice had a mean β la⁺ cell frequency of 1.3% in their lungs, strikingly, TMER-TKO virus-infected mice showed a profound increase in the frequency of infected cells (mean of 7.1%). This phenotype was observed in both the frequency and the number of β la⁺ cells (Fig. 8A to C). Notably, TMER-TKO virus-infected lung samples did not show an overall

increase in the total number of cells recovered compared to WT virus-infected lung samples (Fig. 8D). Although the overall magnitude of infection was much lower in the spleen, TMER-TKO virus-infected mice also showed a parallel increase in the frequency and number of β la⁺ cells in the spleen at this time (Fig. 8E and F), with only a modest increase in the total splenic cellularity of TMER-TKO virus-infected mice (Fig. 8G).

Whereas TMER-TKO virus-infected samples had a profound increase in the frequency of infected cells, infection with the vtRNA1-only γ HV68 virus revealed an intermediate phenotype, in which there was partial restoration of WT values in both the lungs and the spleen (Fig. 8), with a mean frequency of 4.1% β la⁺ cells in the lungs. In sum, these data indicate that the TMERs limit the extent of viral infection in BALB.cIFN- γ ^{-/-} hosts and that the expression of a single vtRNA in the absence of other TMER-associated elements is able to partially reverse this phenotype.

DISCUSSION

ncRNAs regulate a variety of gene expression pathways and cellular processes (36). Despite this, the genetic contribution of many virus-encoded ncRNAs to primary infection has remained unclear. Since the discovery of vtRNA-like elements in the γ HV68 genome (22) and the subsequent identification of hybrid vtRNA-miRNA ncRNAs (6, 23), there has been significant interest in the function of these ncRNAs but little genetic insight (31, 32, 37). Here, we report the generation of viral recombinants completely lacking all eight γ HV68 TMERs, a series of mutations that genetically ablates the expression of eight vtRNA-like elements and all of the associated viral miRNAs.

On the basis of our studies of acute replication *in vitro* and *in vivo*, the γ HV68 TMERs are dispensable for lytic replication *in vitro* and the establishment of latency in B cells in normal, immunocompetent mice. Conversely, the γ HV68 TMERs have a pronounced role in regulating infection and pathogenesis in immunodeficient hosts, as demonstrated by the reduced virulence of the TMER-TKO virus following the infection of BALB.cIFN- γ ^{-/-} hosts. At this time, the precise mechanism(s) by which the TMERs promote pathogenesis in the context of viral pneumonia remains unknown. Notably, the impaired pathogenesis of the TMER-TKO virus is not due to reduced viral replication, since the TMER-TKO has WT levels of viral replication in the lung. This was surprising, given that previous studies demonstrated that attenuated virulence in this model corresponded to a reduced viral titer (35).

One striking effect of infection with the TMER-TKO virus is a pronounced increase in the frequency of virus-infected cells during acute infection. This enhanced frequency of infection is particularly notable because it far exceeds the frequency of infected cells at the peak of viral latency found at early times postinfection. These data indicate an unexpected role for the TMERs in limiting the extent of viral infection at early times postinfection. Despite the increased frequency of infected cells observed in TMER-TKO virus-infected animals, the pathogenesis of the TMER-TKO virus is inversely correlated with the frequency of virus-infected cells. This inverse relationship is further strengthened by the intermediate virulence of the vtRNA1-only recombinant with an intermediate increase in the frequency of infected cells. Future studies will investigate the nature of these infected cells and determine the relationship between the frequency of infected cells and the resulting inflammatory response. It remains to be determined whether

the TMERs have comparable roles in pathogenesis and infection in other states of immunodeficiency.

One of the challenges in understanding the genetic role of the γ HV68 TMERs has been the plethora of TMERs and TMER-derived RNAs. To investigate the possibility of redundancy between TMERs, we generated recombinant viruses that contained only a single TMER (TMER1) or a single vtRNA in the absence of its associated miRNAs (vtRNA1). Strikingly, both the TMER1-only and vtRNA1-only recombinants had a partial restoration of virulence in the induction of lethal pneumonia. Furthermore, analysis of the vtRNA1-only recombinant revealed that the expression of only a single vtRNA, in the absence of the remaining 7 vtRNAs and 15 miRNAs, was capable of partially reversing the enhanced infectivity in BALB.cIFN- γ ^{-/-} hosts. On the basis of these studies, during primary γ HV68 infection, the vtRNA element in the absence of associated miRNAs appears to be a primary functional unit that regulates the extent of infection and pathogenesis. While our lead hypothesis is that the vtRNA is a functional unit, it is possible that the Pol III promoter (internal to vtRNA1) exerts a *cis* regulatory effect on viral gene expression. The phenotype of the vtRNA1 recombinant and the relative contributions of individual miRNA elements in long-term models of infection and pathogenesis remain to be determined.

Our present study has focused on understanding the genetic contribution of the TMER genes, including both vtRNA and miRNA elements, to the early stages of γ HV68 infection. Recently, our collaborators characterized the phenotype of miRNA-deficient γ HV68, generated by deletion of the miRNA stem-loops, leaving only the vtRNA elements intact, followed by an altered, truncated 3' tail (38). Consistent with our results, they found that this mutant virus (i) had nearly WT levels of lytic replication, (ii) can establish latency *in vivo*, and (iii) is impaired in the ability to induce acute lethal pneumonia in immunodeficient mice. They further found that the cellular distribution of the miRNA-deficient γ HV68 virus during latency was perturbed in a dose-dependent manner, with the miRNA-deficient mutant relatively underrepresented in memory B cells. Further studies are required to investigate whether the mutant viruses we have characterized here will reveal similar changes in the latent reservoir; conversely, it remains to be seen if miRNA-deficient γ HV68 has an increased frequency of infected cells, as we have seen for our TMER-TKO virus. Ultimately, it will be important to compare the relative stability and functionality of the vtRNAs among these distinct TMER recombinant viruses.

Though recent research has focused on the role of viral miRNAs as regulators of viral infection (12, 13), it is noteworthy that there is a clear precedent that viral ncRNAs (including the EBV EBERS, the KSHV PAN RNA, the HVS HSURs, and the adenovirus VAs) can have important functional roles in shaping the course of viral infection in the absence of associated miRNAs (3–5, 39). In particular, we are struck by the parallels between the γ HV68 TMERs and the EBV EBERS; both are abundantly expressed, Pol III-dependent small ncRNAs. Previous studies of the EBERS have demonstrated that these RNAs are multifunctional during infection (40), capable of altering innate sensor pathways, including PKR and RIG-I (41, 42), functioning extracellularly (43), and contributing to lymphocyte survival and transformation (40). Though our studies of γ HV68 have focused on parameters different from those studied in the human γ HVs (14–20), our data clearly demonstrate the functional complexity and importance of

γ HV ncRNAs in primary infection *in vivo*. Our data further highlight that ncRNAs might be a new therapeutic target for intervention in γ HV-associated disease.

On the basis of the hybrid nature of the γ HV68 TMERs, we propose that the TMERs may be bifunctional RNAs containing both miRNAs and regulatory ncRNAs, each with their own unique contribution to promoting virus infection and pathogenesis. The capacity of a single vtRNA to partially reverse the phenotypes of the TMER-TKO virus provides clear genetic evidence that the vtRNAs are not simply scaffolds on which miRNAs are hung but are likely functional entities, potentially analogous to the EBERs. Notably, while the vtRNAs are remarkably similar to one another in sequence and structure, the final processed miRNAs have distinct sequences and therefore likely possess specific and unique biological functions. Our data indicate that the TMER-associated vtRNAs have a functional role in γ HV68 acute infection and pathogenesis. Nonetheless, it is worth noting that TMER-derived miRNAs have a tremendous potential for modulating the course of infection. Further genetic studies are required to investigate the contributions of individual TMER-derived miRNAs, with a focus on chronic infection and disease.

In total, our genetic analysis of the γ HV68 TMERs has found that during primary infection *in vivo*, the TMERs promote viral pathogenesis in immunodeficient hosts and regulate the magnitude of viral infection. Further, we provide clear evidence that a single vtRNA can partially rescue the defect resulting from the ablation of all eight TMERs. These data suggest both genetic redundancy among vtRNAs and the existence of bifunctional TMERs, where both the vtRNA and miRNAs are likely to make distinct contributions to infection. The relative contributions of these two classes of ncRNAs to γ HV pathogenesis and their molecular regulation of viral infection remain important areas of investigation.

MATERIALS AND METHODS

Viruses and tissue culture. All viruses and recombinants were derived from γ HV68 strain WUMS (ATCC VR-1465) (44) by using either BAC-derived WT γ HV68 (29) or γ HV68.ORF73 β la (referred to subsequently as γ HV68. β la) (30). For some experiments, γ HV68 Δ 9473 was used (31). Virus stocks used for infection were passaged and grown and their titers were determined on 3T12 cells as previously described (45).

Mouse 3T12 fibroblasts (ATCC CCL-164) were cultured in Dulbecco's modified Eagle medium (DMEM; Life Technologies) supplemented with 5% fetal bovine serum (FBS; Atlanta Biologicals), 2 mM L-glutamine, 10 U/ml penicillin, and 10 μ g/ml streptomycin sulfate (complete DMEM). Vero-Cre cells (gift of David Leib, Dartmouth School of Medicine) were grown in complete DMEM containing 10% FBS.

Plasmids. To prevent transcription of the TMERs, we generated a plasmid in which RNA Pol III promoters spanning the A and B box elements were systematically deleted from each of the eight TMERs by using a previously described strategy (23). This plasmid is referred to as the pHV68-Left End total KO (pLE-TKO) plasmid and is identical to the previously published pLE-KO plasmid (23), with the exception of an additional Pol III promoter mutation introduced into TMER7 by site-directed mutagenesis. After the deletion of TMER7 RNA Pol III promoter elements, the entire pLE-TKO plasmid was sequenced to confirm the proper deletion and absence of off-target point mutations. The primers used for site-directed mutagenesis are described in Table S1 in the supplemental material.

To facilitate disruption of the TMERs by BAC-mediated recombination, we generated the pLE-TKO.Kan^r/I-SceI plasmid, which contains a kanamycin (KAN) resistance (Kan^r) selectable marker and an I-SceI cut

site from the pEPkan-S plasmid (27) inserted into a unique BglII site between *M1* and *M2* in pLE-TKO. This plasmid contains a sequence duplication around the BglII site, an important feature required for scarless removal of the Kan^r selectable marker from BAC DNA. pLE-TKO.Kan^r/I-SceI was generated as follows. In step 1, the Kan^r-encoding gene and the right flanking I-SceI restriction site were PCR amplified from the pEPkan-S plasmid (27) by using primers to generate a sequence duplication surrounding the BglII site in the pLE-TKO plasmid between the *M1* and *M2* ORFs. PCR used the Advantage-HF2 PCR kit with 1 ng of pEPkan-S, 10 pmol of the BglII insert pEPkan-S forward and reverse primers, and 10 \times HF2 PCR buffer in accordance with the manufacturer's protocol (Clontech) (see Table S1 in the supplemental material). The PCR cycling conditions used were (i) a hold at 94°C for 1 min, followed by (ii) 5 cycles of 94°C for 30 s, 53°C for 30 s, and 68°C for 90 s, (iii) 25 cycles of 94°C for 30 s, 58°C for 30 s, and 68°C for 90 s, and (iv) a hold at 68°C for 3 min. PCR amplicons were cloned into the pCR4-TOPO vector (Invitrogen) with constructs confirmed by sequencing. In step 2, to generate the pLE-TKO.Kan^r/I-SceI plasmid, the BglII-Kan^r fragment of the pTOPO-TA.BglII-Kan^r plasmid was cloned into the BglII restriction site of pLE-TKO by standard techniques and confirmed by sequencing.

Generation of electrocompetent and recombination-electrocompetent pGS1783 cells. An overnight culture of *Escherichia coli* strain pGS1783 cells (27, 28) was subcultured in LB medium without drug selection and incubated in a platform shaker at 32°C until the culture reached an optical density at 600 nm (OD₆₀₀) of 0.5 to 0.7. The culture was chilled in an ice bath for 20 min with gentle rocking. Cultures were spun at 4,500 \times g at 4°C for 5 min, after which the cell pellet was resuspended in ice-cold 10% glycerol and washed in cold glycerol. After these two sequential washes, cells were resuspended in ice-cold 10% glycerol, aliquoted into prechilled tubes, and flash frozen in a dry ice-ethanol bath. Cells were stored at -80°C . Recombination-electrocompetent pGS1783 cells were prepared by using the identical methods, with the following modifications. (i) pGS1783 cells were transformed with γ HV68 BAC DNA and grown in LB medium containing 34 μ g/ml of chloramphenicol (CAM). (ii) Following the growth of bacteria to an OD₆₀₀ of 0.5 to 0.7, the culture was incubated for 15 min at 42°C in a shaking water bath prior to being chilled in an ice bath for 20 min with gentle rocking.

Generation of γ HV68 recombinant TMER-TKO viruses. All mutant virus constructs were generated by BAC-mediated recombination by using a modified homologous recombination method based on the use of *E. coli* strain pGS1783 (27, 28). Mutations were introduced into *E. coli* pGS1783 transformed with either WT γ HV68 BAC DNA (29) or WT γ HV68. β la BAC DNA (30). Restriction digest analysis of the BAC DNA isolated from transformed pGS1783 cells confirmed that fully intact, unaltered γ HV68 BAC DNA was present in these cells prior to recombination.

Step 1 was the generation of BAC DNA containing a Kan^r insertion in the TMER locus. Initial disruption of the TMER locus was achieved by the insertion of a Kan^r cassette into the TMER locus. The pLE-TKO.Kan^r/I-SceI plasmid was used as a template for PCR to amplify a 6.1-kb fragment that includes promoter deletions of all eight of the TMER genes, a Kan^r selectable marker, an I-SceI cut site, and a sequence duplication around the BglII site. This PCR product was electroporated into recombination-electrocompetent pGS1783 cells containing either WT γ HV68 or WT γ HV68. β la BAC DNA. The pLE-TKO.Kan^r/I-SceI-derived amplicon was generated with the Pol III miR-M1-1 forward and HV68 pol III-8 Universal reverse primers and the Advantage-HF2 polymerase kit (Clontech). In accordance with the standard Advantage-HF2 PCR protocol, 1.5 ng of template DNA (pLE-TKO.Kan^r/I-SceI) was used to generate the amplicon. The PCR cycling conditions used were (i) a hold at 94°C for 1 min, followed by (ii) 30 cycles of 94°C for 30 s, 51°C for 30 s, and 68°C for 7 min and (iii) a hold at 68°C for 7 min. PCR products were treated with 20 U DpnI (New England Biolabs) for 1 h at 37°C, after which PCR products were resolved on a 0.8% Tris-acetate-EDTA (TAE)-agarose gel, followed by gel purification with the QIAquick gel extraction kit (Qiagen). Gel-

purified PCR products were electroporated with an ECM399 electroporator (BTX) at the HV1500 setting in a chilled 1-mm-gap cuvette into pGS1783 recombination-competent, electrocompetent cells containing either WT γ HV68 or WT γ HV68. β la BAC DNA. Electroporated cells were grown on LB plates with CAM and KAN at 32°C for ~48 h. Kan^r bacteria were screened to identify the γ HV68.Kan^r/I-SceI TMER-TKO and γ HV68. β la.Kan^r/I-SceI TMER-TKO recombinant intermediates (Fig. 2A).

Step 2 was the generation of BAC DNA that contains the TMER-TKO mutation in the absence of the Kan^r-encoding gene. The Kan^r selectable marker was removed from the above-described recombination intermediates. Induction of the I-SceI restriction enzyme in conjunction with the recombination enzymes in pGS1783 cells removed the Kan^r selectable marker from the recombinant intermediates through homologous recombination of the duplication sequences found surrounding the BglII cut site. To do this, pGS1783 cells containing either γ HV68.Kan^r/I-SceI TMER-TKO or γ HV68. β la.Kan^r/I-SceI TMER-TKO BAC DNA were grown in LB-CAM broth overnight at 32°C and then 1-ml volumes of these cultures were subcultured in fresh LB-CAM. After an ~90-min incubation at 32°C, freshly made prewarmed 2% L-arabinose containing LB-CAM broth was added at a 1:1 ratio to the culture and it was incubated for 1 h at 32°C. Cultures were transferred to a 42°C shaking water bath for 30 min and then incubated in a 32°C shaker for ~2.5 h. Bacteria were plated onto a prewarmed 1% L-arabinose LB-CAM plate and incubated at 32°C for ~48 h. Bacteria in which BAC DNA was retained but the Kan^r-encoding gene was deleted by I-SceI induction were identified by replica plating on LB-CAM and LB-KAN plates. Colonies that were CAM insensitive and KAN sensitive were screened via PCR to confirm the loss of the Kan^r selectable marker gene. PCR was conducted with the *Taq* DNA polymerase kit (Qiagen) with the HV68 Left End Seq. #4 Forward, KanR Screen Reverse, and trna6 Reverse primer cocktail. The PCRs were set up in accordance with the *Taq* DNA polymerase manufacturer's protocol. The PCR cycling conditions used were (i) a hold at 95°C for 2 min, followed by (ii) 40 cycles of 94°C for 30 s, 51°C for 30 s, and 72°C for 1 min and (iii) a hold at 72°C for 10 min. Correct genomic structure was verified by restriction digest analysis and direct sequencing of BAC DNA.

The γ HV68. β la TMER1-only BAC DNA construct was generated by an incomplete recombination event during the construction of the γ HV68. β la TMER-TKO BAC DNA. In this recombinant, the TMER1-encoding gene remained intact while promoter deletions recombined into TMER2 through TMER8. Genomic structure was confirmed through restriction digestion of BAC DNA, restriction digestion of a PCR product from the left end of the γ HV68 genome, and direct sequencing of the left end of the γ HV68 genome.

The γ HV68. β la vtRNA1-only BAC DNA was made from the γ HV68 TMER1-only BAC DNA by inserting a termination signal (TTTTTTCCT TTTTT) before the first stem-loop in TMER1 (nucleotides [nt] 203 to 232). This mutation converted an alternative RNA Pol III transcriptional stop element into two canonical RNA Pol III transcriptional termination sequences in tandem separated by 2 nt, an approach we previously used to prevent TMER-derived miRNA production (24). Confirmation of the correct construction of this BAC DNA was achieved through direct sequencing of the left end of the γ HV68 genome.

Following confirmation of the indicated mutations in BAC DNA, we generated infectious virus from these BACs by transfection into 293 cells, followed by virus passage through Vero cells that express cre recombinase, to remove the loxP-flanked BAC origin of replication (46). The absence of the BAC origin of replication from viral DNA was validated by PCR analysis (not shown).

BAC DNA miniprep. Cultures of BAC DNA-containing *E. coli* pGS1783 were grown overnight at 32°C. Cells were then pelleted at 2,200 \times g for 10 min at 4°C. Cells were then sequentially incubated with bacterial lysis buffers P1, P2, and P3 in accordance with the manufacturer's protocol (Qiagen). Bacterial debris was pelleted by centrifugation at 16,000 \times g at room temperature for 10 min. The clarified supernatant was subjected to extraction with a phenol-chloroform-isoamyl alcohol (25:

24:1) solution. A second chloroform extraction (Fisher) was performed, followed by DNA precipitation with 3 M sodium acetate (pH 5.2) and isopropanol and washing with room temperature 70% ethanol. The BAC DNA pellet was air dried at room temperature for 10 min and then resuspended in RNase-free water (Fisher).

RLM-RT-PCR. Viral and cellular miRNAs were amplified by RLM-RT-PCR as previously described (23). RLM-RT-PCR was done with total RNA isolated from infected 3T12 cells (MOI of 5). The product was harvested at 24 or 48 h p.i., and RNA was obtained with the *mirVana* miRNA isolation kit (Ambion). RLM-RT-PCR was done with 10 μ g of RNA combined with 50 ng of either the 5' P or 3' OH-RNA Linker oligonucleotide (see Table S2 in the supplemental material).

Northern blot analysis for small RNAs. Small RNAs were detected by northern blot analysis as previously described (23), with the following modifications. Ten micrograms of total RNA isolated from WT, TKO, vtRNA1-only, or TMER1-only virus-infected or mock-infected 3T12 cells at 24 h was resolved on a 12% denaturing acrylamide gel with 7 M urea. Samples were boiled for 5 min at 95°C, loaded, and run at 30 mA for 1 h. Following imaging of the gel by ethidium bromide staining (23), the gel was transferred at 500 mA for 1 h onto BrightStar Plus positively charged nylon membrane (Ambion) by semidry transfer in 1 \times Tris-borate-EDTA transfer buffer. After transfer, the UV-cross-linked membrane was prehybridized at the hybridization temperature indicated by the probe for 1 h in formamide hybridization buffer (KPL). During prehybridization, the 5'-biotinylated miR-M1-1 RNA probe (5'-biotin-AAAGGAAGUACGGC-CAUUUCUA-3'; genome location, positions 236 to 257), 5'-biotinylated miR-M1-7-3p RNA probe (5'-biotin-AAUAAAGGUGGGCGC-GAUUAUC-3'; genome location, positions 1699 to 1719), 5'-biotinylated miR-M1-14 RNA probe (5'-biotin-AAACGUUCUGCACGCU-GUAGCA-3'; genome location, positions 5141 to 5161), 5'-biotinylated HV68 TMER1 hard stop probe (5'-biotin-AAAGUUGGACCCAC-UUCC-3'; genome location, positions 203 to 221), or HV68 TMER1 stem-loop 2 probe (5'-biotin-AAGAACCUCCGUGUAAUCACU-3'; genome location, positions 298 to 320) was denatured for 10 min at 68°C. The genome coordinates of TMER1 are positions 127 to 322. Following prehybridization, 2.4 μ g of denatured probe was added to the hybridization buffer, which was incubated overnight at the hybridization temperature indicated by the probe.

Following hybridization, the membrane was washed twice with 2 \times SSPE (1 \times SSPE is 0.18 M NaCl, 10 mM NaH₂PO₄, and 1 mM EDTA [pH 7.7])–0.1% SDS, twice with 0.1 \times SSPE–0.1 \times SDS for 15 min at 47°C, and once with 1 \times SSPE at room temperature for 5 min. The biotin-labeled probe was detected with the KPL blotting kit (KPL). The AP-SA conjugate (KPL) was used at a 1:7,000 dilution. The membrane was exposed to Blue Lite Autorad film (ISC BioExpress) for 2 h (23).

SYBR green quantitative RT-PCR analysis. One hundred nanograms of RQ1 DNase-treated total RNA was combined with primers for the amplification of *M1*, *M2*, *M3*, or 18S rRNA (see Table S3 in the supplemental material). RT-PCR mixtures consisted of RNA, primers, and the iScript One-Step RT-PCR with SYBR green kit (Bio-Rad). RT-PCR was done on an iCycler (Bio-Rad) with the following cycles: (i) a hold at 50°C for 10 min, (ii) a hold at 95°C for 5 min, and (iii) 45 cycles of 95°C for 10 s and 56°C for 30 s. A melting curve analysis was done as follows: 95°C for 1 min, 55°C for 1 min, and 55°C for 10 s for 80 cycles with a 0.5°C decrease every cycle.

RT-PCR amplification. The PCR primers used are listed in Table S2 in the supplemental material. RT-PCR and no-RT control reactions were performed in a 25- μ l volume containing a final primer concentration of 0.5 μ M with either the OneStep RT-PCR kit (Qiagen) or the *Taq* polymerase (1,000 U) kit (Qiagen), respectively. Prior to amplification, 1 μ g of total RNA was treated with 2 U of RQ1 RNase-Free DNase (Promega). One hundred nanograms of RQ1 DNase-treated RNA was used as the template for amplification in the RT-PCR and no-RT amplification reactions. RT-PCR cycles were as follows: (i) 30 min at 50°C, followed by 15 min at 95°C, (ii) 35 amplification cycles of 30 s at 94°C, 30 s at 51 to 61°C (dependent on the *T_m* of each primer set), and 30 s at 72°C, and (iii)

a 5-min hold at 72°C. No-RT reactions were identical to the RT-PCR conditions, except that prior to the 35 amplification cycles there was a single incubation for 3 min at 95°C. All PCR products were resolved on 2% TAE-agarose gels and visualized by ethidium bromide staining.

Viral replication analysis. NIH 3T12 fibroblasts were infected at an MOI of 5 for single-step replication analysis or an MOI of 0.05 for multistep replication analysis as previously described (47). Samples (cells and supernatant) were harvested at 0, 6, 12, 24, and 48 h p.i. for single-step analysis and at 0, 24, 48, 72, and 144 h p.i. for multistep analysis. Samples were subjected to three freeze-thaw cycles prior to quantitation by plaque assay (35).

Mice. B6 mice (stock no. 000664) were purchased from the Jackson Laboratory (Bar Harbor, ME). BALB/c.IFN- $\gamma^{-/-}$ mice, originally obtained from the Jackson Laboratory [strain C.129S7(B6)-Ifngtm1Ts/J, stock no. 002286], were bred in house at the University of Colorado Denver Anschutz Medical Campus in accordance with university regulations. Mice were infected between 8 and 16 weeks of age. All infected mice were housed in an animal biosafety level 2 facility in accordance with all university regulations.

Virus infection of mice. Mice were inoculated intranasally at 4×10^5 PFU/mouse with either WT γ HV68 or the indicated viral recombinants in a 40- μ l total volume of complete medium and harvested at the indicated time postinfection. Mice were monitored daily for signs of disease, and any mice that appeared moribund were sacrificed, and their lungs, hearts, and spleens were removed for histologic and molecular analyses (35).

Ex vivo viral titer analysis. Infected tissues were removed and collected at the indicated time postinfection and frozen at -80°C . After one freeze-thaw cycle, 1 ml of complete medium was added to each tissue with 1.0-mm silica beads (BioSpec Products Inc. catalog no. 11079110z) and tissues were homogenized via FastPrep FP120 (Thermo Savant). Sample viral titers were determined by plaque assay on 3T12 fibroblasts (47).

Histology. Lungs were removed from euthanized mice and submerged in a 10% buffered formalin phosphate solution (Fisher Scientific). Tissues were placed in fresh formalin 24 to 72 h postfixation and then submitted to the University of Colorado Denver Cancer Center histology facility. Tissues were paraffin embedded, and tissue sections were stained with hematoxylin and eosin prior to analysis by a pathologist (C.D.C.).

Flow cytometric analysis. Infected lungs and spleens were analyzed at the postinfection times indicated. Lungs were harvested from mice that had been previously perfused with phosphate-buffered saline; this was followed by tissue mincing and enzymatic digestion with collagenase D (from *Clostridium histolyticum*; Roche) for 1 h at 37°C (48). Following digestion, lungs were mechanically disrupted into single-cell suspensions over 100- μ m nylon filters and resuspended for staining. Spleens were mechanically disrupted into single-cell suspensions and subjected to red blood cell lysis. To identify β -lactamase expression, 6×10^6 cells were incubated with the β -lactamase substrate CCF2-AM (1 mM; Invitrogen, Life Technologies) in accordance with the manufacturer's directions. Cells were then stained with fluorescently conjugated antibodies against CD44 (eBioscience clone eBioIM7), CD19 (eBioscience clone eBio1D3), and IgD (BioLegend clone 11-26c.2a). All staining was done in the presence of Fc receptor-blocking antibody 2.4G2. Flow cytometric analysis was performed on an LSR II flow cytometer (BD Biosciences). Compensation values were calculated with the DIVA software (BD Biosciences), and compensation values were based on fluorescence values obtained with antibody-stained compensation beads.

Software and statistical analysis. Data analysis and plotting were done with Prism 6.0d (GraphPad Software, Inc., San Diego, CA). Statistical analyses were performed with Prism 6.0d and assessed by unpaired *t* test or one-way analysis of variance (ANOVA) and Dunnett's multiple-comparison test, and the *P* values obtained are shown. In the case of survival curves, statistical analysis was done by log-rank (Mantel-Cox) test. Flow cytometric data were analyzed with FlowJo (TreeStar, Inc., Ashland, OR), and the data are displayed as dot plots showing outliers on \log_{10} scales.

Ethics statement. This study was carried out in accordance with the recommendations in the Guide for the Care and Use of Laboratory Animals of the National Institutes of Health. All animal studies were conducted in

accordance with the University of Colorado Denver Institutional Animal Use and Care Committee under the Animal Welfare Assurance of Compliance policy (no. a3269-01). All procedures were performed under isoflurane anesthesia, and all efforts were made to minimize suffering.

SUPPLEMENTAL MATERIAL

Supplemental material for this article may be found at <http://mbio.asm.org/lookup/suppl/doi:10.1128/mBio.01670-14/-DCSupplemental>.

Table S1, PPT file, 0.2 MB.

Table S2, PPTX file, 0.1 MB.

Table S3, PPT file, 0.2 MB.

ACKNOWLEDGMENTS

We thank N. Osterrieder for the kind gift of pGS1783 cells and the pEPkan-S plasmid for BAC recombineering, the ClinImmune flow cytometry core, the University of Colorado Cancer Center Histology core, the Center for Comparative Medicine, and members of the van Dyk laboratory for critical discussion.

This research was funded by a Burroughs Wellcome Investigators in the Pathogenesis of Infectious Disease grant and National Institutes of Health grants R01CA168558 and R56AI091994 to L.F.V. and 2T32NS7321-21A1 to K.W.D and American Heart Association National Scientist Development Award (#13SDG14510023) to E.T.C. These studies were supported by core services through NIH/NCATS Colorado CTSI grant UL1 TR001082 and University of Colorado Cancer Center P30CA046934. The contents of this report are our sole responsibility and do not necessarily represent official NIH views. We have no competing financial interests to declare.

REFERENCES

- Speck SH, Virgin HW. 1999. Host and viral genetics of chronic infection: a mouse model of gamma-herpesvirus pathogenesis. *Curr Opin Microbiol* 2:403–409. [http://dx.doi.org/10.1016/S1369-5274\(99\)80071-X](http://dx.doi.org/10.1016/S1369-5274(99)80071-X).
- Cesarman E. 2011. Gammaherpesvirus and lymphoproliferative disorders in immunocompromised patients. *Cancer Lett* 305:163–174. <http://dx.doi.org/10.1016/j.canlet.2011.03.003>.
- Conrad NK, Fok V, Cazalla D, Borah S, Steitz JA. 2006. The challenge of viral snRNPs. *Cold Spring Harb Symp Quant Biol* 71:377–384. <http://dx.doi.org/10.1101/sqb.2006.71.057>.
- Takada K. 2001. Role of Epstein-Barr virus in Burkitt's lymphoma. *Curr Top Microbiol Immunol* 258:141–151. http://dx.doi.org/10.1007/978-3-642-56515-1_9.
- Sun R, Lin SF, Gradoville L, Miller G. 1996. Polyadenylated nuclear RNA encoded by Kaposi sarcoma-associated herpesvirus. *Proc Natl Acad Sci U S A* 93:11883–11888. <http://dx.doi.org/10.1073/pnas.93.21.11883>.
- Pfeffer S, Sewer A, Lagos-Quintana M, Sheridan R, Sander C, Grässer FA, van Dyk LF, Ho CK, Shuman S, Chien M, Russo JJ, Ju J, Randall G, Lindenbach BD, Rice CM, Simon V, Ho DD, Zavolan M, Tuschl T. 2005. Identification of microRNAs of the herpesvirus family. *Nat Methods* 2:269–276. <http://dx.doi.org/10.1038/nmeth746>.
- Samols MA, Hu J, Skalsky RL, Renne R. 2005. Cloning and identification of a microRNA cluster within the latency-associated region of Kaposi's sarcoma-associated herpesvirus. *J Virol* 79:9301–9305. <http://dx.doi.org/10.1128/JVI.79.14.9301-9305.2005>.
- Cai X, Lu S, Zhang Z, Gonzalez CM, Damania B, Cullen BR. 2005. Kaposi's sarcoma-associated herpesvirus expresses an array of viral microRNAs in latently infected cells. *Proc Natl Acad Sci U S A* 102:5570–5575. <http://dx.doi.org/10.1073/pnas.0408192102>.
- Grundhoff A, Sullivan CS, Ganem D. 2006. A combined computational and microarray-based approach identifies novel microRNAs encoded by human gamma-herpesviruses. *RNA* 12:733–750. <http://dx.doi.org/10.1261/rna.2326106>.
- Zhu JY, Strehle M, Frohn A, Kremmer E, Höfig KP, Meister G, Adler H. 2010. Identification and analysis of expression of novel microRNAs of murine gammaherpesvirus 68. *J Virol* 84:10266–10275. <http://dx.doi.org/10.1128/JVI.01119-10>.
- Reese TA, Xia J, Johnson LS, Zhou X, Zhang W, Virgin HW. 2010. Identification of novel microRNA-like molecules generated from herpes-

- virus and host tRNA transcripts. *J Virol* 84:10344–10353. <http://dx.doi.org/10.1128/JVI.00707-10>.
12. Zhu Y, Haecker I, Yang Y, Gao SJ, Renne R. 2013. Gamma-herpesvirus-encoded miRNAs and their roles in viral biology and pathogenesis. *Curr Opin Virol* 3:266–275. <http://dx.doi.org/10.1016/j.coviro.2013.05.013>.
 13. Zhu Y, Huang Y, Jung JU, Lu C, Gao SJ. 2014. Viral miRNA targeting of bicistronic and polycistronic transcripts. *Curr Opin Virol* 7:66–72. <http://dx.doi.org/10.1016/j.coviro.2014.04.004>.
 14. Yajima M, Kanda T, Takada K. 2005. Critical role of Epstein-Barr virus (EBV)-encoded RNA in efficient EBV-induced B-lymphocyte growth transformation. *J Virol* 79:4298–4307. <http://dx.doi.org/10.1128/JVI.79.7.4298-4307.2005>.
 15. Feederle R, Linnstaedt SD, Bannert H, Lips H, Bencun M, Cullen BR, Delecluse HJ. 2011. A viral microRNA cluster strongly potentiates the transforming properties of a human herpesvirus. *PLoS Pathog.* 7:e1001294. <http://dx.doi.org/10.1371/journal.ppat.1001294>.
 16. Rossetto CC, Pari G. 2012. KSHV PAN RNA associates with demethylases UTX and JMJD3 to activate lytic replication through a physical interaction with the virus genome. *PLoS Pathog.* 8:e1002680. <http://dx.doi.org/10.1371/journal.ppat.1002680>.
 17. Moody R, Zhu Y, Huang Y, Cui X, Jones T, Bedolla R, Lei X, Bai Z, Gao SJ. 2013. KSHV microRNAs mediate cellular transformation and tumorigenesis by redundantly targeting cell growth and survival pathways. *PLoS Pathog.* 9:e1003857. <http://dx.doi.org/10.1371/journal.ppat.1003857>.
 18. Swaminathan S, Tomkinson B, Kieff E. 1991. Recombinant Epstein-Barr virus with small RNA (EBER) genes deleted transforms lymphocytes and replicates *in vitro*. *Proc Natl Acad Sci U S A* 88:1546–1550. <http://dx.doi.org/10.1073/pnas.88.4.1546>.
 19. Ensser A, Pfänder A, Müller-Fleckenstein I, Fleckenstein B. 1999. The URNA genes of herpesvirus saimiri (strain C488) are dispensable for transformation of human T cells *in vitro*. *J Virol* 73:10551–10555.
 20. Wahl A, Linnstaedt SD, Esoda C, Krisko JF, Martinez-Torres F, Delecluse HJ, Cullen BR, Garcia JV. 2013. A cluster of virus-encoded microRNAs accelerates acute systemic Epstein-Barr virus infection but does not significantly enhance virus-induced oncogenesis *in vivo*. *J Virol* 87:5437–5446. <http://dx.doi.org/10.1128/JVI.00281-13>.
 21. Barton E, Mandal P, Speck SH. 2011. Pathogenesis and host control of gammaherpesviruses: lessons from the mouse. *Annu Rev Immunol* 29:351–397. <http://dx.doi.org/10.1146/annurev-immunol-072710-081639>.
 22. Bowden RJ, Simas JP, Davis AJ, Efstathiou S. 1997. Murine gammaherpesvirus 68 encodes tRNA-like sequences which are expressed during latency. *J Gen Virol* 78:1675–1687.
 23. Diebel KW, Smith AL, van Dyk LF. 2010. Mature and functional viral miRNAs transcribed from novel RNA polymerase III promoters. *RNA* 16:170–185. <http://dx.doi.org/10.1261/rna.1873910>.
 24. Diebel KW, Claypool DJ, van Dyk LF. 2014. A conserved RNA polymerase III promoter required for gammaherpesvirus TMER transcription and microRNA processing. *Gene* 544:8–18. <http://dx.doi.org/10.1016/j.gene.2014.04.026>.
 25. Bogerd HP, Karnowski HW, Cai X, Shin J, Pohlers M, Cullen BR. 2010. A mammalian herpesvirus uses noncanonical expression and processing mechanisms to generate viral microRNAs. *Mol Cell* 37:135–142. <http://dx.doi.org/10.1016/j.molcel.2009.12.016>.
 26. Orioli A, Pascali C, Quartararo J, Diebel KW, Praz V, Romascano D, Percudani R, van Dyk LF, Hernandez N, Teichmann M, Dieci G. 2011. Widespread occurrence of non-canonical transcription termination by human RNA polymerase III. *Nucleic Acids Res* 39:5499–5512. <http://dx.doi.org/10.1093/nar/gkr074>.
 27. Tischer BK, von Einem J, Kaufer B, Osterrieder N. 2006. Two-step red-mediated recombination for versatile high-efficiency markerless DNA manipulation in *Escherichia coli*. *Biotechniques* 40:191–197. <http://dx.doi.org/10.2144/000112096>.
 28. Tischer BK, Smith GA, Osterrieder N. 2010. En passant mutagenesis: a two step markerless red recombination system. *Methods Mol Biol* 634:421–430. http://dx.doi.org/10.1007/978-1-60761-652-8_30.
 29. Adler H, Messerle M, Wagner M, Koszinowski UH. 2000. Cloning and mutagenesis of the murine gammaherpesvirus 68 genome as an infectious bacterial artificial chromosome. *J Virol* 74:6964–6974. <http://dx.doi.org/10.1128/JVI.74.15.6964-6974.2000>.
 30. Nealy MS, Coleman CB, Li H, Tibbetts SA. 2010. Use of a virus-encoded enzymatic marker reveals that a stable fraction of memory B cells expresses latency-associated nuclear antigen throughout chronic gammaherpesvirus infection. *J Virol* 84:7523–7534. <http://dx.doi.org/10.1128/JVI.02572-09>.
 31. Clambey ET, Virgin HW, Speck SH. 2002. Characterization of a spontaneous 9.5-kilobase-deletion mutant of murine gammaherpesvirus 68 reveals tissue-specific genetic requirements for latency. *J Virol* 76:6532–6544. <http://dx.doi.org/10.1128/JVI.76.13.6532-6544.2002>.
 32. Macrae AI, Dutia BM, Milligan S, Brownstein DG, Allen DJ, Mistrikova J, Davison AJ, Nash AA, Stewart JP. 2001. Analysis of a novel strain of murine gammaherpesvirus reveals a genomic locus important for acute pathogenesis. *J Virol* 75:5315–5327. <http://dx.doi.org/10.1128/JVI.75.11.5315-5327.2001>.
 33. Flaño E, Kim IJ, Woodland DL, Blackman MA. 2002. Gamma-herpesvirus latency is preferentially maintained in splenic germinal center and memory B cells. *J Exp Med* 196:1363–1372. <http://dx.doi.org/10.1084/jem.20020890>.
 34. Willer DO, Speck SH. 2003. Long-term latent murine gammaherpesvirus 68 infection is preferentially found within the surface immunoglobulin D-negative subset of splenic B cells *in vivo*. *J Virol* 77:8310–8321. <http://dx.doi.org/10.1128/JVI.77.15.8310-8321.2003>.
 35. Lee KS, Cool CD, van Dyk LF. 2009. Murine gammaherpesvirus 68 infection of gamma interferon-deficient mice on a BALB/c background results in acute lethal pneumonia that is dependent on specific viral genes. *J Virol* 83:11397–11401. <http://dx.doi.org/10.1128/JVI.00989-09>.
 36. Cech TR, Steitz JA. 2014. The noncoding RNA revolution—trashing old rules to forge new ones. *Cell* 157:77–94. <http://dx.doi.org/10.1016/j.cell.2014.03.008>.
 37. Simas JP, Bowden RJ, Paige V, Efstathiou S. 1998. Four tRNA-like sequences and a serpin homologue encoded by murine gammaherpesvirus 68 are dispensable for lytic replication *in vitro* and latency *in vivo*. *J Gen Virol* 79:149–153.
 38. Feldman ER, Kara M, Coleman CB, Grau KR, Oko LM, Krueger BJ, Renne R, van Dyk LF, Tibbetts SA. 2014. Virus-encoded microRNAs facilitate gammaherpesvirus latency and pathogenesis *in vivo*. *mBio* 5:e00981-00914. <http://dx.doi.org/10.1128/mBio.00981-14>.
 39. Dzananovic E, Patel TR, Deo S, McEleney K, Stetefeld J, McKenna SA. 2013. Recognition of viral RNA stem-loops by the tandem double-stranded RNA binding domains of PKR. *RNA* 19:333–344. <http://dx.doi.org/10.1261/rna.035931.112>.
 40. Iwakiri D, Takada K. 2010. Role of EBERs in the pathogenesis of EBV infection. *Adv Cancer Res* 107:119–136. [http://dx.doi.org/10.1016/S0065-230X\(10\)07004-1](http://dx.doi.org/10.1016/S0065-230X(10)07004-1).
 41. Nanbo A, Inoue K, Adachi-Takasawa K, Takada K. 2002. Epstein-Barr virus RNA confers resistance to interferon-alpha-induced apoptosis in Burkitt's lymphoma. *EMBO J* 21:954–965. <http://dx.doi.org/10.1093/emboj/21.5.954>.
 42. Samanta M, Iwakiri D, Kanda T, Imaizumi T, Takada K. 2006. EB virus-encoded RNAs are recognized by RIG-I and activate signaling to induce type I IFN. *EMBO J* 25:4207–4214. <http://dx.doi.org/10.1038/sj.emboj.7601314>.
 43. Iwakiri D, Zhou L, Samanta M, Matsumoto M, Ebihara T, Seya T, Imai S, Fujieda M, Kawa K, Takada K. 2009. Epstein-Barr virus (EBV)-encoded small RNA is released from EBV-infected cells and activates signaling from Toll-like receptor 3. *J Exp Med* 206:2091–2099. <http://dx.doi.org/10.1084/jem.20081761>.
 44. Virgin HW, Latreille P, Wamsley P, Hallsworth K, Weck KE, Dal Canto AJ, Speck SH. 1997. Complete sequence and genomic analysis of murine gammaherpesvirus 68. *J Virol* 71:5894–5904.
 45. Suárez AL, van Dyk LF. 2008. Endothelial cells support persistent gammaherpesvirus 68 infection. *PLoS Pathog.* 4:e1000152. <http://dx.doi.org/10.1371/journal.ppat.1000152>.
 46. Lee KS, Suarez AL, Claypool DJ, Armstrong TK, Buckingham EM, van Dyk LF. 2012. Viral cyclins mediate separate phases of infection by integrating functions of distinct mammalian cyclins. *PLoS Pathog.* 8:e1002496. <http://dx.doi.org/10.1371/journal.ppat.1002496>.
 47. van Dyk LF, Virgin HW, Speck SH. 2000. The murine gammaherpesvirus 68 v-cyclin is a critical regulator of reactivation from latency. *J Virol* 74:7451–7461. <http://dx.doi.org/10.1128/JVI.74.16.7451-7461.2000>.
 48. Ehrentraut H, Westrich JA, Eltzschig HK, Clambey ET. 2012. Adora2b adenosine receptor engagement enhances regulatory T cell abundance during endotoxin-induced pulmonary inflammation. *PLoS One* 7:e32416. <http://dx.doi.org/10.1371/journal.pone.0032416>.
 49. Kozomara A, Griffiths-Jones S. 2011. miRBase: integrating microRNA annotation and deep-sequencing data. *Nucleic Acids Res* 39:D152–D157. <http://dx.doi.org/10.1093/nar/gkq1027>.